Catechin, a green tea component, rapidly induces apoptosis of myeloid leukemic cells via modulation of reactive oxygen species production *in vitro* and inhibits tumor growth *in vivo*

Tomonori Nakazato
Keisuke Ito
Yoshitaka Miyakawa
Kentaro Kinjo
Taketo Yamada
Nobumichi Hozumi
Yasuo Ikeda
Masahiro Kizaki

Background and Objectives. The aim of this study was to investigate the possibility of green tea polyphenol, (-)-epigallocatechin-3-gallate (EGCG) as a novel therapeutic agent for patients with myeloid leukemia.

Design and Methods. We investigated the effects of EGCG on the induction of apoptosis in leukemic cells *in vitro* and *in vivo*. We further examined the molecular mechanisms of EGCG-induced apoptosis in myeloid leukemic cells.

Results. EGCG rapidly induced apoptotic cell death in retinoic acid (RA)-resistant acute promyelocytic leukemia (APL), UF-1 cells within 3 h. EGCG-induced apoptosis in UF-1 cells was associated with the loss of mitochondrial transmembrane potentials ($\Delta\Psi_m$) and activation of caspase-3 and -9. Elevation of intracellular reactive oxygen species (ROS) production was also demonstrated during EGCG-induced apoptosis of UF-1 as well as fresh myeloid leukemic cells. In NOD/SCID mice transplanted with UF-1 cells, EGCG effectively inhibited tumor growth *in vivo*, and the number of mitoses among the cells significantly decreased in comparison to the number in control mouse cells.

Interpretation and Conclusions. In summary, EGCG has potential as a novel therapeutic agent for myeloid leukemia via induction of apoptosis mediated by modification of the redox system.

Key words: green tea, catechin, apoptosis, leukemic cells, reactive oxygen species.

Haematologica 2005; 90:317-325

From the Division of Hematology, Department of Internal Medicine (TN, KI, YM, KK, YI, MK) and Pathology, Keio University School of Medicine, Tokyo, Japan (TY); Institute of Biological Science, Science University of Tokyo, Chiba, Japan (NH).

Correspondence:
Masahiro Kizaki, M.D.,
Division of Hematology, Department of Internal Medicine, Keio University School of Medicine, 35 Shinanomachi, Shinjuku-ku, Tokyo 160-8582, Japan.
E-mail: makizaki@sc.itc.keio.ac.jp

Recently, green tea has attracted much attention because of its beneficial health effects; the polyphenolic compounds present in green tea include (-)-epigallocatechin-3-gallate (EGCG), (-)-epicatechin-3-gallate (ECG), (-)-epigallocatechin (EGC), and epicatechin (EC), which have been shown to have cancer preventive effects in many animal tumor models.[1] In fact, epidemiologic studies have shown that green tea consumption can reduce the incidence of cancer and metastases.[2-6] Green tea has unique characteristics as an agent and has few adverse effects. In addition, it is inexpensive, can be consumed orally, and has a long history as a generally tolerated beverage among all races. Therefore, green tea appears to have the potential of becoming an ideal agent for chemoprevention.[7] Moreover, EGCG has been shown to induce G_0/G_1 phase cell cycle arrest in human epidermoid carcinoma cells, thereby inhibiting proliferation and inducing apoptosis in many cancer cells *in vitro*.[7-9] The therapeutic approach to acute leukemia is basically chemotherapy to achieve complete remission, based on the concept of *total cell killing*.[10] However, severe side effects and complications such as serious infections and bleeding due to anti-cancer drugs are major problems in the clinical setting. In addition, repeated episodes of relapse of the disease may lead to refractory or chemotherapy-resistant leukemia. The clinical evidence thus suggests the limitations of leukemia chemotherapy; novel effective therapeutic approaches with less toxicity are therefore actively being sought. Differentiation-inducing therapy employing a physiologically active derivative of vitamin A, all-*trans* retinoic acid (ATRA), brought remarkable advances in the therapeutic outcomes of acute promyelocytic leukemia (APL) at the end of the last century.[11] However, the clinical remission due to ATRA is of short duration, and most patients who receive continuous treatment with ATRA develop RA-resistant diseases.[12] Therefore, investigators have actively sought out new agents with the ability to stimulate cellular differentiation and induce apoptosis in the types of cells associated with acute leukemia.

Design and Methods

Cells and cell culture

The RA-resistant APL cell line UF-1 was established in our laboratory from a patient with relapsed APL who had received ATRA,[13] and the RA-sensitive NB4 promyelocytic leukemia cell line was a gift from Dr. M. Lanotte (Hôpital St Louis, Paris, France).[14] The human myeloid leukemic cell lines HL-60, U937, K562, and KU812 were obtained from the Japan Cancer Research Resources Bank (Tokyo, Japan). Bone marrow or peripheral blood samples from 6 newly diagnosed patients with acute myelogenous leukemia (AML) were obtained according to appropriate Human Protection Committee validation and with informed consent. Mononuclear cells were separated by Lymphoprep (Nycomed Pharma As, Oslo, Norway). The percentage of leukemic blast cells was more than 80% of the mononuclear cells. Cells were maintained in RPMI 1640 medium (GIBCO-BRL, Gaitherburg, MD, USA) with 15% fetal calf serum (Hyclone Laboratories, Logan, MT, USA), 100 U/mL penicillin, and 100 mg/mL streptomycin in a humidified atmosphere with 5% CO_2.

Reagents

Various catechin derivatives, including EC, ECG, EGC, and EGCG, were purchased from WAKO Chemical Co. (Tokyo, Japan). Catechin derivatives were dissolved in DMSO and none of the cultures contained more than 0.1% DMSO. Controls were run using 0.1% DMSO and this concentration of diluent had no effect. N-acetyl-L-cysteine (NAC), rotenone, and myxothiazol were obtained from Sigma Chemical Co. (St. Louis, MO, USA).

Assays for apoptosis

Apoptotic cells were quantified by annexin V-FITC and propidium iodide (PI) double staining using a staining kit purchased from PharMingen (San Diego, CA, USA). In addition, induction of apoptosis was detected by a DNA fragmentation assay. The mitochondrial transmembrane potential ($\Delta\psi_m$) was determined by flow cytometry (FACS Calibur; Becton Dickinson, San Jose, CA, USA). Briefly, cells were washed twice with PBS and incubated with 1 μg/mL rhodamine 123 (Sigma) at 37° for 30 min. Rhodamine 123 intensity was determined by flow cytometry.

Cell cycle analysis

Cells (1×10^6) were suspended in hypotonic solution (0.1% Triton X-100, 1 mM Tris-HCl (pH 8.0), 3.4 mM sodium citrate, 0.1 mM EDTA) and stained with 50 μg/mL of PI. The DNA content was analyzed by flow cytometry. The population of cells in each cell cycle phase was determined using ModiFIT software (Becton Dickinson).

Caspase assays

In the caspase inhibitor assay, cells were pretreated with a synthetic pan-caspase inhibitor (20 μM, Z-VAD-FMK) or caspase-3 inhibitor (50 μM, DEVD-CHO), and caspase-8 and -9 inhibitors (50 μM, Z-IETD-FMK and LEHD-CHO, respectively) for 2 h prior to addition of EGCG (100 μM). All inhibitors were purchased from Calbiochem (La Jolla, CA, USA).

Measurement of intracellular generation of ROS

To assess the generation of reactive oxygen species (ROS), control and EGCG-treated cells were incubated with 5 μM DHE (Molecular Probes, Eugene, OR, USA), which is oxidized to the fluorescent intercalator, ethidium, by cellular oxidants, particularly superoxide radicals. Cells (5×10^5) were stained with 5 μM DHE for 30 min at 37°C, and were then washed and resuspended in PBS. The oxidative conversion of DHE to ethidium was measured by flow cytometry (Becton Dickinson).

Cell lysate preparation and Western blotting

Cells were collected by centrifugation at 700 g for 10 min and then the pellets were resuspended in lysis buffer (1% NP-40, 1 mM phenylmethylsulfonyl fluoride (PMSF), 40 mM Tris-HCl (pH8.0), 150 mM NaCl) at 4°C for 15 min. For the detection of PML/RARα, cells were extracted by the method of Yoshida *et al.*[15] Mitochondrial and cytosolic fractions were prepared with digitonin-nagarse treatment. Protein concentrations were determined using a protein assay DC system (Bio-Rad, Richmond, CA, USA). Cell lysates (15 μg protein per lane) were fractionated in 12.5% SDS-polyacrylamide gels prior to transfer to the membranes (Immobilon-P membranes, Millipore, Bedford, MA, USA) using a standard protocol.

Antibody binding was detected by using an enhanced chemiluminescence kit for Western blotting detection with hyper-electrochemiluminescence film (Amersham, Buckinghamshire, UK). Blots were stained with Coomassie brilliant blue to confirm that there were equal amounts of protein extract on each lane. The following antibodies were used in this study: anti-caspase 3, -cytochrome *c* (PharMingen, San Diego, CA, USA), -Bcl-2, -BAX, -Bcl-X_L, -$p21^{CIP1/WAF1}$, -$p27^{KIP1}$, β-actin, -RARα, -Mcl-1, -survivin (Santa Cruz Biotech, Santa Cruz, CA), -cleaved PARP (Cell Signalling Technology, Inc., Beverly, MA, USA), and –Smac/DIABLO (MBL, Nagoya, Japan).

Animal model and experimental design

We have established the first human ATRA-resistant APL model in an NOD/SCID mice system using UF-1 cells.[16] Briefly, mice were pretreated with 3 Gy of total body irradiation, which is a sublethal dose that was expected to enhance the acceptance of xenografts. Subsequently, UF-1 cells (1×10^7 cells) in their logarith-

mic growth phase were inoculated subcutaneously into NOD/SCID mice (Jackson Laboratory, Bar Harbor, ME, USA). Inoculated UF-1 cells formed subcutaneous tumors at the injection site, and cells grew rapidly. Forty days after implantation of the cells, mice with the transplanted cells were randomly assigned to receive water (n=5) or 10 mM EGCG (n=5) as the sole drinking fluid administered daily for 12 days. After 12 days of treatment, mice were sacrificed and dissected to measure tumor weights. When the mice showed severe wasting or when observations were finished, they were sacrificed according to the UKCCCR guidelines, and the day of sacrifice was recorded.[17] Tumors were removed, fixed in 4% paraformaldehyde, and embedded in paraffin. Sections through the tumor were cut by a cryostat, and were mounted on glass slides for histological staining with hematoxylin and eosin. Mitotic cells in the same fields were counted in sections from both control and EGCG-treated animals, and expressed as the number of mitoses per field.

Statistical analysis

Tumor weights and the number of mitotic cells are expressed as mean ± SD. Differences in both parameters were analyzed for significance by Student's *t* test. $p<0.05$ was considered as statistically significant.

Results

Catechin inhibited cellular proliferation of various leukemic cells

We first examined whether the green tea polyphenols and the polyphenolic epicatechin derivatives induced inhibition of the growth of leukemic cells, including NB4, UF-1, HL-60, K562, and U937 cells. The structurally related catechins, i.e., EC, ECG, EGC and EGCG, inhibited the growth of leukemic cells. However, EGCG was the most potent inhibitor among the 4 derivatives (Figure 1). We thus used EGCG for the series of experiments. Treatment with EGCG for 24 h induced a marked inhibition of UF-1 cell growth and, to a lesser but significant extent, led to an inhibition of cellular growth in all other myeloid leukemic cells (Figure 2A). Among the cells tested, UF-1 cells were the most sensitive to EGCG with an IC50 of 50 μM (Figure 2A). Therefore, we used UF-1 cells for the further experiments.

EGCG induced G1 cell cycle arrest and subsequent apoptosis

The effects of EGCG on cell cycle progression were investigated using UF-1 cells. The cells were treated with 100 μM EGCG for 24 h and analyzed for cell cycle distribution by means of flow cytometry. Culture with EGCG increased the population of cells in the G1 phase from 69.9% to 91.0%, with a reduction of cells in the S phase from 27.7% to 7.5% (Figure 2B). In addition, a strong induction of apoptosis was shown by the appearance of a haplodiploid DNA peak with sub-G1 DNA contents at 24 h after treatment (Figure 2B). These results indicate that EGCG led to cell cycle arrest at the G1 phase followed by apoptosis. We thus confirmed the induction of apoptosis by EGCG by means of DNA ladder formation and annexin V/PI staining. Interestingly, DNA ladder formation was confirmed at a time point as early as 3 h by electrophoresis of genomic DNA extracted from UF-1 cells treated with 100 μM EGCG (Figure 2C). Consistent with these results, the numbers of annexin V-positive cells increased after incubation with EGCG for 3 h (Figure 2D), thus indicating that EGCG rapidly induced apoptosis in UF-1 and NB4 cells.

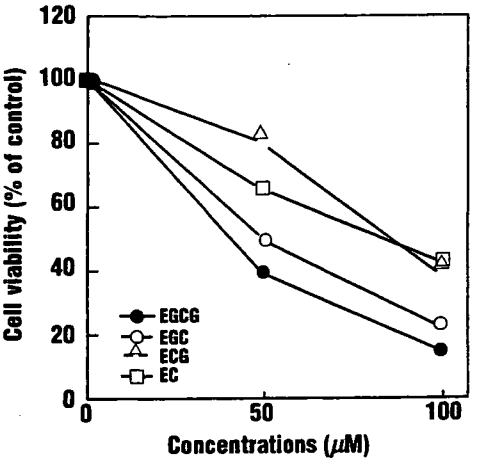

Figure 1. Effect of catechin derivatives on UF-1 cells. UF-1 cells were treated for 24 hours with the indicated dose of the major green tea polyphenols: (-)-epicatechin (EC), (-)-epicatechin-3-gallate (ECG), (-)-epigallocatechin (EGC), and (-)-epigallocatechin-3-gallate (EGCG). Cell viability was assessed by trypan blue dye exclusion. EGCG is the most potent inhibitor of leukemic cell growth.

Effects of EGCG on caspase-3 activity

To address the apoptotic pathway in EGCG-treated UF-1 cells, we next examined the activation of caspase-3 by Western blot analysis using antibody that recognizes both active and inactive forms of caspase-3. The 32-kDa procaspase-3 was cleaved into active forms (17kDa) after just 1 h of exposure to EGCG (100 μM) (Figure 3A). In addition, significant PARP cleavage was detected by 6 h of treatment with EGCG (Figure 3A). Furthermore, to elucidate the functional role of caspases in EGCG-induced apoptosis, experiments were performed with a series of caspase inhibitors. UF-1 cells were treated with 100 μM EGCG for 24 h, either alone or in combination with Z-VAD-FMK (pan caspase inhibitor), DEVD-CHO (caspase-3-specific inhibitor),

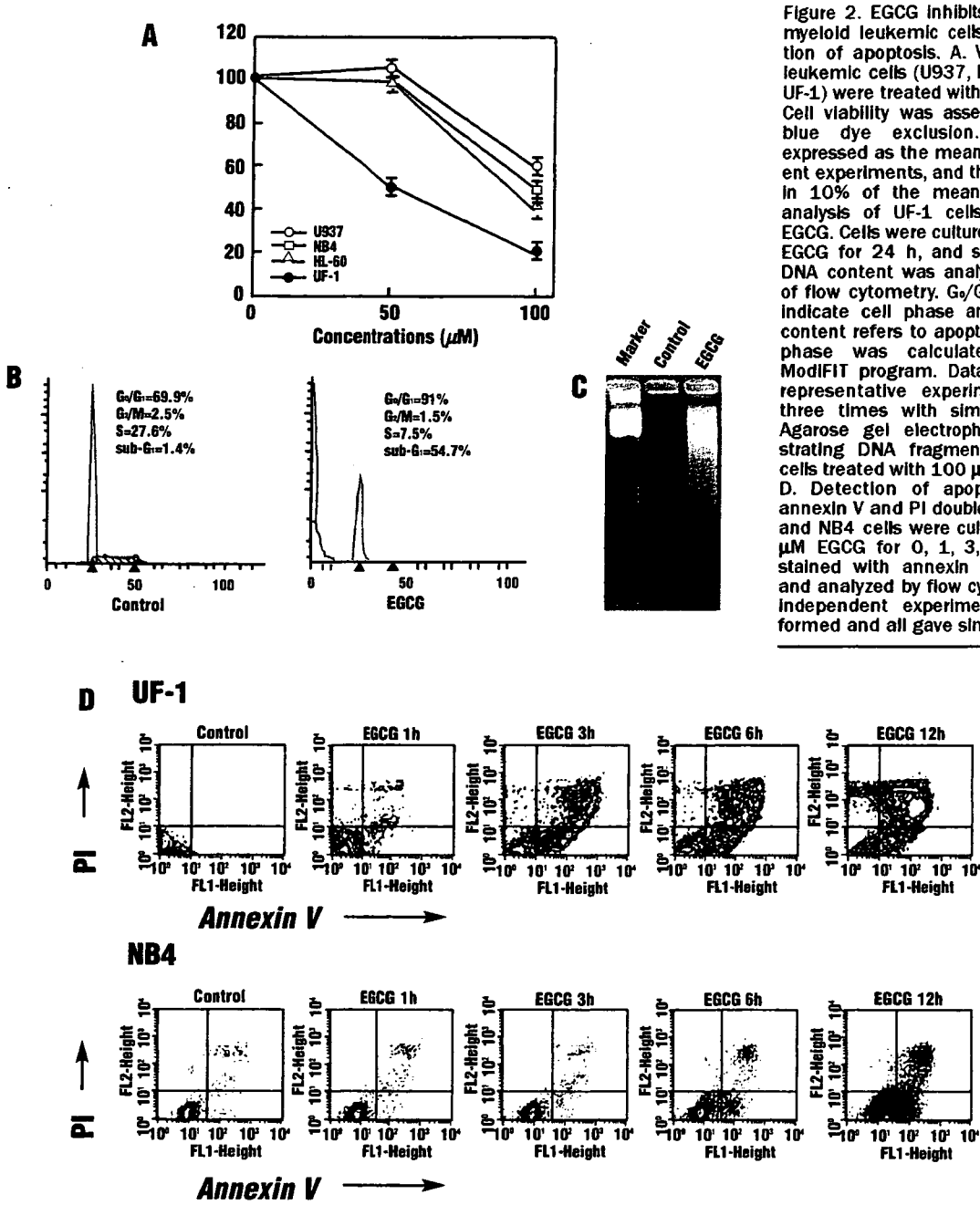

Figure 2. EGCG inhibits the growth of myeloid leukemic cells via the induction of apoptosis. A. Various myeloid leukemic cells (U937, NB4, HL-60 and UF-1) were treated with EGCG for 24 h. Cell viability was assessed by trypan blue dye exclusion. Results are expressed as the mean of three different experiments, and the SD was within 10% of the mean. B. Cell cycle analysis of UF-1 cells cultured with EGCG. Cells were cultured with 100 μM EGCG for 24 h, and stained with PI. DNA content was analyzed by means of flow cytometry. G_0/G_1, G_2/M, and S indicate cell phase and sub-G_1 DNA content refers to apoptotic cells. Each phase was calculated using the ModiFIT program. Data shown are a representative experiment repeated three times with similar results. C. Agarose gel electrophoresis demonstrating DNA fragmentation in UF-1 cells treated with 100 μM EGCG for 3h. D. Detection of apoptotic cells by annexin V and PI double staining. UF-1 and NB4 cells were cultured with 100 μM EGCG for 0, 1, 3, 6, and 12 h, stained with annexin V-FITC and PI, and analyzed by flow cytometry. Three independent experiments were performed and all gave similar results.

Z-IETD-FMK (caspase-8-specific inhibitor), or LEHD-CHO (caspase-9-specific inhibitor). EGCG-induced apoptosis was completely blocked by treatment with Z-VAD-FMK, DEVD-CHO, and LEHD-CHO, but not caspase-8-specific inhibitor, Z-IETD-FMK (Figure 3C). These results suggest that EGCG-induced apoptosis is associated with the activation of caspase-3 and -9, but not of caspase-8.

Expression of apoptosis-associated proteins

The expression of Bax protein was increased in a time-dependent manner by treatment with EGCG in UF-1 cells (Figure 4A). In contrast, EGCG did not modulate the levels of anti-apoptotic Bcl-2 and Bcl-X_L proteins in UF-1 cells. However, Bcl-2 family Mcl-1 and survivin were down-regulated after 6 h of EGCG treatment (Figure 4A). Expression of cdk inhibitors ($p21^{CIP1/WAF1}$ and $p27^{KIP1}$) was rapidly increased after 1 h exposure of EGCG in UF-1 cells (Figure 4B). UF-1 is a cell line from a patient with APL who had the chromosomal abnormality t(15;17), resulting in a *PML/RARA* fusion gene; this chimeric gene and its product may play important roles in leukemogenesis and development of this specific type of leukemia.[18] Therefore, we

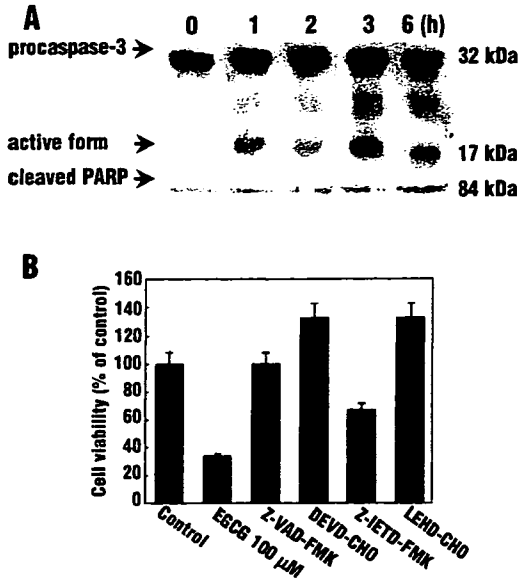

Figure 3. Effects of EGCG on caspase activation. A. Western blot analysis of caspase-3 and cleaved PARP. Total cellular proteins (15 μg per each lane) were separated on 12.5% SDS- polyacrylamide gels and transferred to the membrane. Protein levels of caspase-3 were detected by Western blot analysis using antibody against caspase-3. Treatment with EGCG (100 μM) induced processing of caspase-3 (32 kDa), indicated by the appearance of a 17 kDa cleaved active form. The anti-cleaved PARP antibody recognized cleaved PARP (84 kDa) in EGCG-treated UF-1 cells. Coomassie brilliant blue stain was used to confirm that each lane contained equal amounts of protein. B. Effects of caspase inhibitors on EGCG-treated UF-1 cells. Inhibition of EGCG-induced apoptosis of UF-1 cells was estimated in a co-culture with a series of caspase inhibitors. Cells were preincubated with each caspase inhibitor for 2 h prior to addition of 100 μM EGCG. Results are expressed as the mean ± SD of three different experiments. Z-VAD-FMK, pan caspase inhibitor; DEVD-CHO, caspase-3 inhibitor; Z-IETD-FMK, caspase-8 inhibitor; and LEHD-CHO, caspase-9 inhibitor.

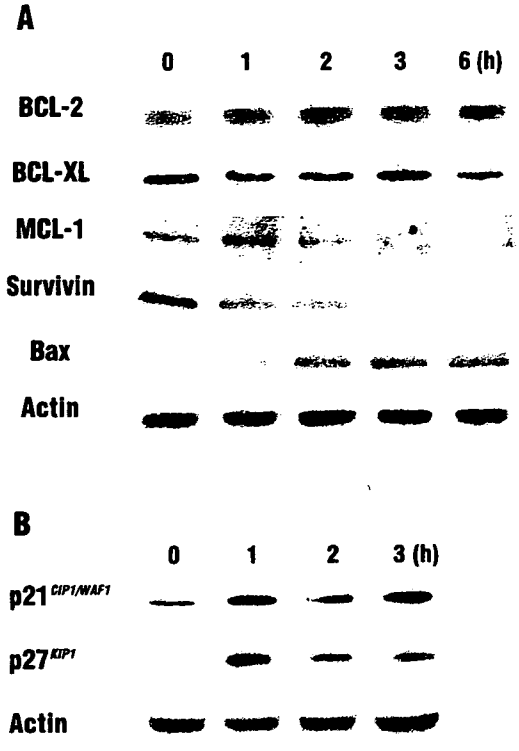

Figure 4. Expressions of the apoptosis-associated proteins and CDK inhibitors. A. UF-1 cells were treated with 100 μM EGCG for the indicated time. Cell lysates (15 μg per each lane) were fractionated on 12.5% SDS-polyacrylamide gels and analyzed by Western blotting with antibodies against Bcl-2, Bcl-X_L, MCl-1, survivin, Bax and β-actin proteins. B. The protein level of CDK inhibitors ($p21^{CIP1/WAF1}$, $p27^{KIP1}$) was detected by Western blotting. Re-blotting with β-actin staining demonstrated that equal amounts of protein were present in each lane.

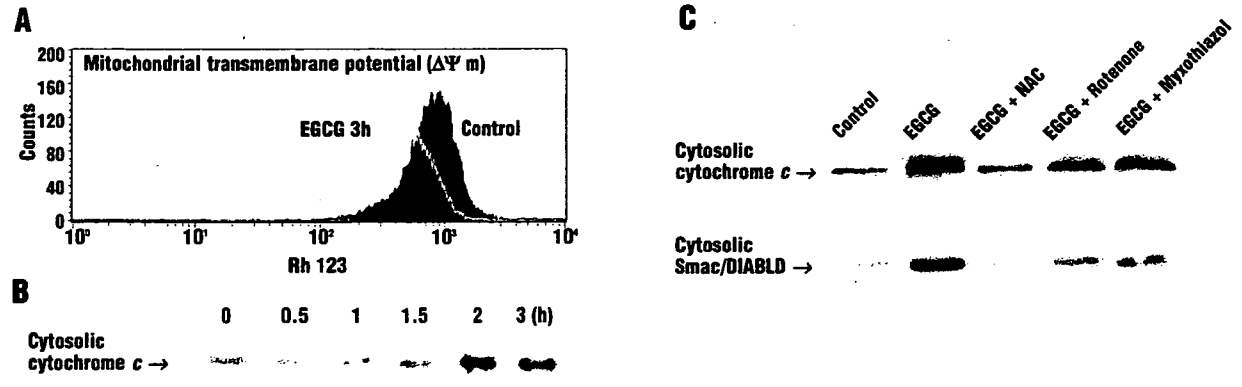

Figure 5. EGCG-induced apoptosis occurred via the mitochondrial pathway. A. Flow cytometric analysis of mitochindrial ΔΨm, as estimated by rhodamine 123 intensity. UF-1 cells were cultured with 100 μM EGCG for 3 hours, and rhodamine 123 fluorescence was analyzed by flow cytometry. B. Western blot analysis of cytochrome c in EGCG-treated UF-1 cells. Cells were incubated with 100 μM EGCG for the indicated time. The arrow indicates the expression of cytosolic cytochrome *c*. C. Effects of antioxidant and MRC inhibitors on the release of cytochrome *c* and Smac/DIABLO from the mitochondria to the cytosol during EGCG-induced apoptosis in UF-1 cells. UF-1 cells were pre-treated with NAC (10 mM), rotenone (1 μM), myxothiazol (100 nM) for 1 h, followed by the treatment of 100 μM EGCG for 3 h. The release of cytochrome c and Smac/DIABLO was analyzed by Western blotting.

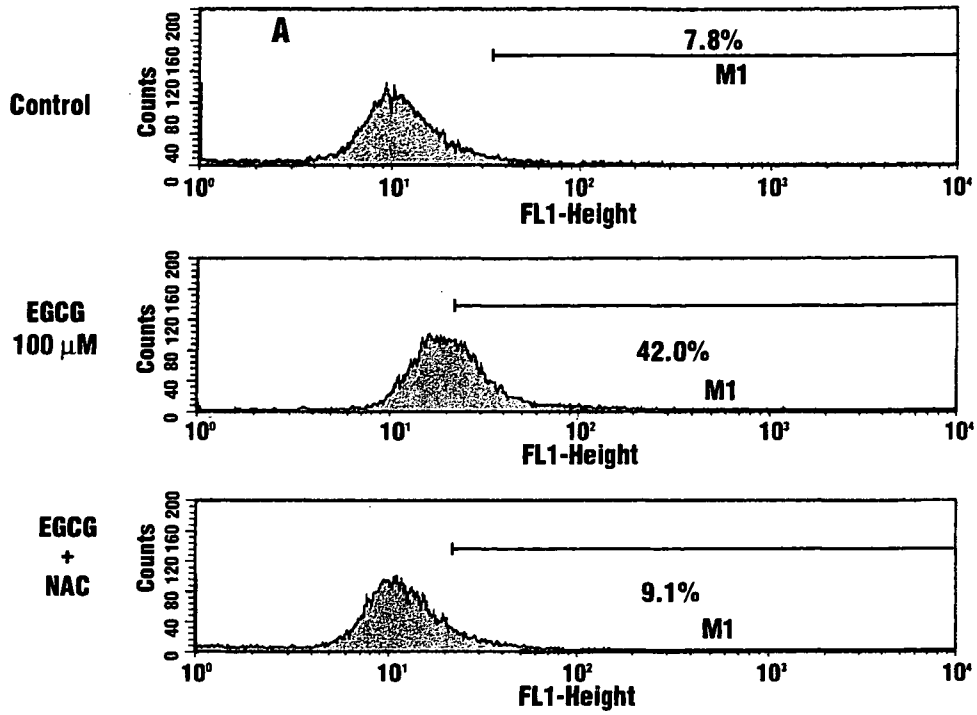

Figure 6. ROS generation by EGCG in UF-1 cells. To determine the intracellular concentration of ROS, UF-1 cells were cultured with DHE, and the fluorescence was measured by flow cytometry. DHE-derived fluorescence in untreated UF-1 cells and in cultures treated for 3 h with 100 μM EGCG is shown at the top and in the lower panel, respectively.

analyzed the effect of EGCG on this disease-specific chimeric protein. EGCG did not induce degradation of the PML/RARα chimeric protein (*data not shown*), suggesting that EGCG-induced apoptosis in UF-1 cells is not involved in the *PML/RARA* signaling pathway.

EGCG-induced death signaling is mediated through the mitochondrial pathway

Mitochondrial changes, including permeability transition pore opening and the collapse of $\Delta\psi_m$, result in the release of cytochrome c into the cytosol, which subsequently causes apoptosis by the activation of caspases.[19] After treatment with 100 μM EGCG for 3 h, low Rh123 staining in UF-1 cells indicated an increase in the loss of $\Delta\psi_m$ (Figure 5A). The loss of $\Delta\psi_m$ appeared in parallel with the activation of caspase-3 and -9, as well as with apoptosis. In addition, EGCG induced a substantial release of cytochrome c from the mitochondria into the cytosol in a time-dependent manner in UF-1 cells (Figure 5B). These results suggest that mitochondrial dysfunction causes the release of cytochrome *c* into the cytosol; caspase-9 and -3 were then activated, thereby propagating the death signal. The major sources of ROS are components of the mitochondrial respiratory chain (MRC). We also examined the role of the MRC components in EGCG-induced apoptosis in UF-1 cells by using MRC inhibitors, rotenone and myxothiazol. Antioxidant, NAC, completely inhibited the release of cytochtome c and Smac/DIABLO from the mitochondria into the cytosol, but MRC inhibitors caused partial inhibition (Figure 5C).

ROS production triggers EGCG-induced apoptosis

Several investigators have reported that EGCG-induced apoptosis is often associated with the generation of ROS.[6,20] We therefore analyzed the production of intracellular ROS in control and EGCG-treated cells. Treatment of UF-1 cells with 100 μM EGCG for 3 h caused dramatic oxidation of DHE to ethidium, and resulted in the induction of intracellular ROS (Figure 6A). Furthermore, treatment of UF-1 cells with a thiol antioxidant, NAC, an excellent supplier of glutathione (GSH), completely blocked generation of intracellular ROS and EGCG- induced apoptosis in UF-1 cells (Figure 6A and *data not shown*). Our data indicate that the modulation of molecules involved in the redox system, particularly that of the GSH, may determine the sensitivity of leukemia cells to EGCG. Furthermore, we examined the effect of EGCG on induction of apoptosis and ROS production in fresh leukemia cells from 6 patients with AML. These results were consistent with the results obtained from the previously mentioned cell lines, i.e., sensitivity to EGCG-induced apoptosis was

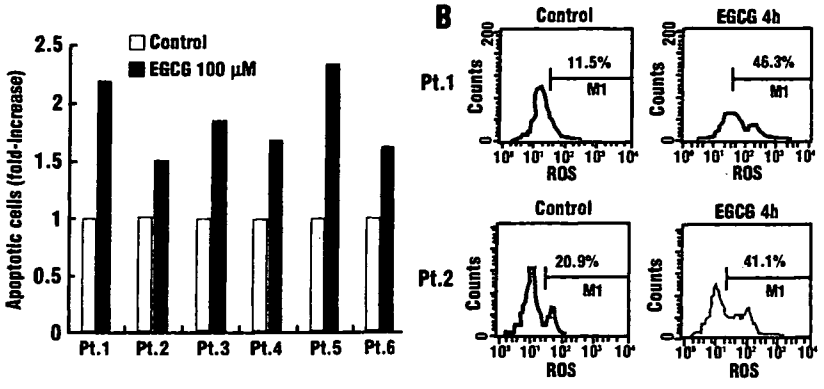

Figure 7. Effects of EGCG on fresh leukemic samples from patients with AML. Leukemic cells were separated by the Lymphoprep sedimentation procedure and subsequently cultured with 100 μM EGCG for 4 h. A. Apoptosis was evaluated by annexin V and PI double staining and showed the fold-increase of apoptotic cells in each case. B. Intracellular levels of ROS were measured by flow cytometry in representative EGCG-sensitive (Pt 1) and -less sensitive (Pt 2) cases. EGCG-sensitive leukemic cells are defined as those in which the increase of ROS production with treatment of EGCG is more than two-fold that in control cells.

observed in fresh leukemia cells from patients, and similarly increased production of intracellular ROS was also observed (Figure 7A and B). ROS production was 4.0 and 1.9-fold increased in EGCG-sensitive and -less sensitive fresh myeloid leukemic cells from the patients (patients 1 and 2, respectively) (Figure 7B).

EGCG induces apoptosis in vivo

Our *in vitro* data prompted us to examine whether the effects of EGCG are equally valid *in vivo*. After 40 days of implantation of UF-1 cells into NOD/SCID mice, water, used as a control (n=5), or 10 mM EGCG (n=5) treatment were administered orally as the sole drinking fluid ingested daily for 12 days. We found that tumor weight was significantly lower in the mice that were given EGCG compared to in the mice treated with water as a control ($p<0.05$, mean weight: 1.52g in the EGCG-treated group vs. 2.20g in the control group) (Figure 8A). During the treatment, the EGCG-treated mice appeared healthy and continued to eat. In addition, pathologic analysis at autopsy revealed no EGCG-induced tissue changes in any of the organs (*data not shown*). These results suggest that EGCG had no toxic effects on mice during the treatment. Tumor cell proliferation was evaluated by counting the number of mitoses. Comparing the number of mitoses by hematoxylin and eosin staining in the same fields, a significantly lower number was observed in the EGCG group ($p<0.001$, Figure 8B), suggesting that cell proliferation was more inhibited in the EGCG-treated mice than in the control mice.

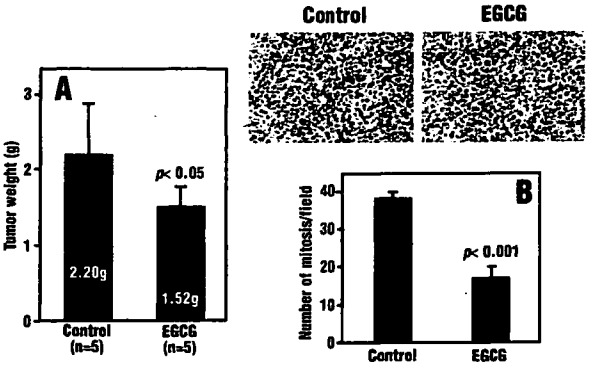

Figure 8. EGCG-mediated apoptosis of leukemic cells *in vivo* using an NOD/SCID mice model. A. UF-1 cells (1×10^7 cells) were inoculated subcutaneously into NOD/SCID mice. Forty days after transplantation, water (control) or 10 mM EOGCG was given as the sole drinking fluid daily for 12 days. After 12 days of treatment, mice were sacrificed and tumor weights were measured. Values shown are mean ± SD (*bars*). B. The tumor sections were fixed and stained with hematoxylin and eosin. The number of mitosis in the same fields was counted in both control and EGCG-treated tumor sections. Arrows indicate cells with mitoses. Values shown are mean ± SD (*bars*). Original magnification, × 100.

Discussion

Extensive *in vitro* cell culture studies, as well as *in vivo* studies in animal models, have verified the cancer preventive effects of green tea, and specifically, of its individual polyphenols.[21] Epidemiological studies, though inconclusive, have suggested that green tea may reduce the risks associated with many cancers including bladder, prostate, esophageal and gastric carcinomas.[2-6] Green tea extracts, especially its major polyphenolic component EGCG, are capable of inhibiting the growth of a variety of mouse and human cancer cells via the induction of *in vitro* apoptosis.[1,22,23] However, the precise mechanism of EGCG-induced apoptosis remains to be elucidated. In this study, we demonstrated that one green tea component in particular, EGCG, suppressed the cellular growth of various fresh leukemic cells and myeloid leukemia cell lines, especially promyelocytic UF-1 cells. The observed growth inhibition of leukemic cells was due to the induction of apoptosis. Mitochondria play an essential role in death signal transduction such that permeability tran-

sition pore opening and collapse of the $\Delta\psi_m$ resulted in the rapid release of caspase activators such as cytochrome *c* into the cytoplasm.[24] We demonstrated that the loss of the $\Delta\psi_m$ increased within 3 h of treatment, a time frame parallel to that of induced apoptosis. Furthermore, caspase-3 was activated by EGCG, and caspase-3 and caspase-9 inhibitors suppressed the apoptotic effects of EGCG. Taken together, these results suggest that EGCG-induced apoptosis in leukemic cells is associated with the loss of $\Delta\psi_m$ and with the activation of caspases, probably via the cytochrome *c*/Apaf-1/caspase-9 pathway. We further demonstrated that EGCG had no influence on the expression of Bcl-2 and Bcl-X_L, but it up-regulated the levels of Bax protein, and down-regulated the levels of Mcl-1 and survivin in UF-1 cells in a time-dependent manner. We detected that EGCG-induced apoptosis in UF-1 cells and in certain fresh leukemia samples was associated with an increase in the levels of intracellular ROS. It has been suggested that the generation of ROS is a common mechanism in one of the representative pathways of apoptosis.[20] Oxidants are capable of depleting GSH and damaging the cellular antioxidant defense system, and can directly induce apoptosis.[25-27] On the other hand, antioxidants such as NAC can inhibit apoptosis. Interestingly, a recent study using cDNA microarrays has identified that superoxide dismutases (SOD) are target molecules of estrogen-induced apoptosis in leukemic cells, and inhibition of SOD causes an accumulation of ROS and leads to the release of cytochrome *c* from the mitochondria.[28] Although EGCG is generally well-known as an antioxidant, it can also behave as a pro-oxidant under certain conditions.[6,29] Therefore, we hypothesized that EGCG-induced apoptosis is also related to the GSH redox system, in a manner similar to the As_2O_3-induced apoptosis in APL cells.[30,31] An antioxidant, NAC, increased intracellular GSH contents and completely blocked EGCG-induced apoptosis. In contrast, MRC inhibitors, rotenone and myxothiazol, partially blocked EGCG-induced cytochrome *c* and Smac/DIABLO release from the mitochondria to the cytosol, suggesting that MRC is required for the induction of apoptosis of the leukemic cells via mitochondrial ROS production by treatment with EGCG. EGCG was able to induce G1 cell cycle arrest in the leukemic cells. The loss of cell cycle checkpoints in cancer cells confers a growth advantage.[32-34] Therefore, EGCG suppresses cell growth by imposing cell cycle checkpoints in leukemic cells. To clarify the mechanisms of EGCG effects on the cell cycle, we examined the expression of cell cycle-associated proteins, including CDK, CDK inhibitors and various cyclins by Western blot analysis. Expression of $p21^{CIP1/WAF1}$ and $p27^{KIP1}$ increased in a time-dependent manner, whereas the expression of cyclin D1, cyclin E, CDK2, and CDK4 were not altered by EGCG (*data not shown*). Up-regulation of $p21^{CIP1/WAF1}$ and $p27^{KIP1}$ may thus play a pivotal role in inducing cell cycle arrest and apoptosis in EGCG-treated UF-1 cells. Recent studies have also indicated that green tea is an effective inhibitor of angiogenesis *in vivo*.[35,36]

Catechin, a component of green tea, is a natural compound, and it appears to be safer than current chemotherapeutic drugs. Since we could not observe any organ damage *in vivo*, catechin might be developed as a new potent anti-cancer agent for the management of hematologic malignancies. In particular, it might be useful in older patients or in immunocompromised patients because of its safety and lack of known toxicity. Since green tea extracts have already entered phase I trials in patients with solid tumors in the USA,[37] it would be useful to design similar clinical trials with leukemic patients to evaluate its anti-leukemic effects. In conclusion, this component of green tea may have potential as a novel therapeutic agent to replace or augument the more cytotoxic agents currently used to treat the patients with leukemia.

TN: performed the research and wrote the first version of the paper; KI: performed FACS analysis; YM, KK: planned in vivo experiments and managed patients; TY, NH: performed in vivo experiments and histological analyses; AI: collected patients' samples and analyzed clinical data; MK: designed the whole research and wrote the final version of this manuscript. The authors declare that they have no potential conflict of interest.

This work was supported in part by grants from the Ministry of Education, Culture, Sports, Science, and Technology of Japan; the Keio University Medical Science Fund from Keio University; and the Chamber of Commerce in Green Tea of Kyoto Prefecture in Japan.

Manuscript received May 11, 2004. Accepted January 7, 2005

References

1. Yang CS, Wang ZY. Tea and cancer (review). J Natl Cancer Inst 1993;85: 1038-49.
2. Asano Y, Okamura S, Ogo T, Eto T, Otsuka T, Niho Y. Effect of (-)-epigallocatechin gallate on leukemic blast cells from patients with acute myeloblastic leukemia. Life Sci 1997; 60:135-42.
3. Lea MA, Xiao Q, Sadhukhan AK, Cottle S, Wang ZY, Yang CS. Inhibitory effects of tea extracts and (–)-epigallocatechin gallate on DNA synthesis and proliferation of hepatoma and erythroleukemia cells. Cancer Lett 1996;68:231-6.
4. Valcic S, Timmermann BN, Alberts DS, Wachter GA, Kurtzsch M, Wymer J, et al. Inhibitory effect of six green tea catechins and caffeine on the growth of four selected human tumor cell lines. Anticancer Drugs 1996;7:461-8.
5. Liao S, Umekita Y, Guo J, Kokontis JM, Hiipakka RA. Growth inhibition and regression of human prostate and breast tumors in athymic mice by epigallocatechin gallate. Cancer Lett 1995;25:239-43.
6. Islam S, Islam N, Kermode T, Johnstone B, Mukhtar H, Moskowitz RW, et al. Involvement of caspase-3 in epigallocatechin-3-gallate-mediated apoptosis of human chondrosarcoma cells. Biochem Biophys Res Commun 2000;270:793-7.
7. Ahmad N, Feyes DK, Nieminen AL, Agarwal R, Mukhtar H. Green tea constituent epigallocatechin-3-gallate and induction of apoptosis and cell cycle arrest in human carcinoma cells. J Natl Cancer Inst 1997;89:1881-6.
8. Lepley DM, Li B, Birt DF, Pelling JC. The chemopreventive flavonoid api-

genin induces G2/M arrest in keratinocytes. Carcinogenesis 1996; 17: 2367-75.
9. Ahmad N, Cheng P, Mukhtar H. Cell cycle dysregulation by green tea polyphenol epigallocatechin-3-gallate. Biochem Biophys Res Commun 2000; 275:328-34.
10. Skipper HE. Thoughts on cancer chemotherapy and combination modality therapy. JAMA 1974;230:1033-5.
11. Tallman MS, Nabhan C, Feusner JH, Rowe JM. Acute promyelocytic leukemia: evolving therapeutic strategies. Blood 2001;99:759-67.
12. Warrell RP Jr. Retinoid resistance in acute promyelocytic leukemia: new mechanisms, strategies, and implications. Blood 1993;82:1941-53.
13. Kizaki M, Matsushita H, Takayama N, Muto A, Ueno H, Awaya N, et al. Establishment and characterization of a novel acute promyelocytic leukemia cell line (UF-1) with retinoic acid-resistant features. Blood 1996;88:1824-33.
14. Lanotte M, Martin-Thouvenin V, Najman S, Balerini P, Valensi F, Berger R. NB4, a maturation inducible cell line with t(15;17) marker isolated from a human acute promyelocytic leukemia (M3). Blood 1991;77:1080-6.
15. Yoshida H, Kitamura K, Tanaka K, Omura S, Miyazaki T, Hachiya T, et al. Accelerated degradation of PML-retinoic acid receptor α (PML-RARA) oncoprotein by all-trans retinoic acid in acute promyelocytic leukemia: possible role of the proteasome pathway. Cancer Res 1996; 56:2945-8.
16. Fukuchi Y, Kizaki M, Kinjo K, Awaya N, Ito M, Kawai Y, et al. Establishment of a retinoic acid-resistant human acute promyelocytic leukemia (APL) model in human granulocyte-macrophage colony-stimulating factor (hGM-CSF) transgenic severe combined immunodeficiency (SCID) mice. Br J Cancer 1998;78:878-84.
17. Workman P, Balman A, Hickman JA, McNally NJ, Mitchison NA, Pierrepoint CG, et al. UKCCCR guidelines for the welfare of animals in experimental neoplasia. Br J Cancer 1988; 58:109-13.
18. Costoya JA, Pandolfi PP. The role of promyelocytic leukemia zinc finger and promyelocytic leukemia in leukemogenesis and development. Curr Opin Hematol 2001;8:212-7.
19. Green DR, Reed JC. Mitochondria and apoptosis. Science 1998;281:1309-12.
20. Yang G, Liao J, Kim K, Yurkow EJ, Yang CS. Inhibition of growth and induction of apoptosis in human cancer cells by tea polyphenols. Carcinogenesis 1998; 19:611-6.
21. Nam S, Smith DM, Dou QP. Ester bound-containing tea polyphenols potently inhibit proteasome activity in vitro and in vivo. J Biol Chem 2001; 276:13322-30.
22. Ahmad N, Gupta S, Mukhtar H. Green tea polyphenol epigallocatechin-3-gallate differentially modulates nuclear factor κB in cancer cells versus normal cells. Arch Biochem Biophys 2000; 376:338-46.
23. Gupta S, Ahmad N, Nieminen AL, Mulhtar H. Growth inhibition, cell-cycle dysregulation, and induction of apoptosis by green tea constituent (-)-epigallocatechin-3-gallate in androgen-sensitive and androgen-insensitive human prostate carcinoma cells. Toxicol Appl Pharmacol 2000;164:82-90.
24. Li P, Nijhawan D, Budihardjo J, Srinivasula SM, Ahmad M, Alnewri ES, et al. Cytochrome c and ATP-dependent formation of Apaf-1/caspase-9 complex initiates an apoptotic proteasome cascade. Cell 1997; 91: 479-89.
25. Troyano A, Fernandez C, Sancho P, de Blas E, Aller P. Effect of glutathione depletion on antitumor drug toxicity (apoptosis and necrosis) in U937 human promyelocytic cells. J Biol Chem 2001;276:47107-1.
26. Albina JE, Cui S, Mateo RB, Reiehner JS. Nitric oxide-mediated apoptosis in murine peritoneal macrophages. J Immunol 1993;150:5080-5.
27. Pervaiz S, Ramalingam JK, Hirpara JL, Clement M. Superoxide anion inhibits drug-induced tumor cell death. FEBS Lett 1999;459:343-8.
28. Huang P, Feng P, Oldham EA, Keating MJ, Plunkett W. Superoxide dismutases as a target for the sensitive killing of cancer cells. Nature 2000;407:390-5.
29. Sergediene E, Jönsson K, Szymusiak H, Tyrakowska B, Rietjens IMCM, Cenas N. Prooxidant toxicity of polyphenolic antioxidants to HL-60 cells: description of quantitative structure-activity relationship. FEBS Lett 1999;462:392-6.
30. Dai J, Weinberg RS, Waxman S, Jing Y. Malignant cells can be sensitized to undergo growth inhibition and apoptosis by arsenic trioxide through modulation of the glutathione redox system. Blood 1999;93:268-77.
31. Jing Y, Dai J, Chalmens-Redman RME, Tatton WG, Waxman S. Arsenic trioxide selectively induces acute promyelocytic leukemia cell apoptosis via a hydrogen peroxide-dependent pathway. Blood 1999;94:2102-11.
32. Hartwell LH, Kastan MB. Cell cycle control and cancer. Science 1994; 266: 1821-8.
33. Dulic V, Kaufmann WK, Wilson SJ, Tlsty TD, Lee SE, Harper JW, et al. p53-dependent inhibition of cyclin-dependent kinase activities in human fibroblasts during radiation-induced G1 arrest. Cell 1994;76:1013-23.
34. Liu M, Pelling JC. UV-B/A irradiation of mouse keratinocytes results in p53-mediated WAF1/CIP1 expression. Oncogene 1995;10:1955-60.
35. Bertolini F, Fusetti L, Cinieri S, Martinelli G, Pruneri G. Inhibition of angiogenesis and induction of endothelial and tumor cell apoptosis by green tea in animal models of human high-grade non-Hodgkin's lymphoma. Leukemia 2000;14:1477-82.
36. Lamy S, Gingras D, Béliveau R. Green tea catechins inhibit vascular endothelial growth factor receptor phosphorylation. Cancer Res 2002;62:381-5.
37. Pisters AMW, Newman RA, Coldman B, Shin DM, Khuri FR, Hong WK, et al. Phase I trial of oral green tea extract in adult patients with solid tumors. J Clin Oncol 2001;19:1830-8.

Pathology International 2005; **55**: 504–509

Case report

Primary bone carcinosarcoma: Chondrosarcoma and squamous cell carcinoma with keratin pearl formation

Junichi Shiraishi,[1] Makio Mukai,[1] Hiroo Yabe,[2] Rie Shibata,[3] Taketo Yamada,[3] Keiko Miura,[2] Ukei Anazawa,[2] Hideo Morioka[2] and Michiie Sakamoto[3]

Departments of [1]Diagnostic Pathology, [2]Orthopaedic Surgery and [3]Pathology, Keio University School of Medicine, Tokyo, Japan

Malignant bone tumors with epithelial differentiation are extremely rare. Only one case of primary malignant bone tumor with distinct squamous cell carcinoma and chondrosarcoma has ever been reported. Reported herein is a case of primary malignant bone tumor with distinct squamous cell carcinoma and chondrosarcoma, so-called carcinosarcoma of bone, arising in the femur of a 53-year-old man. The tumor was located within the femur and was diagnosed by curettage as a well-differentiated chondrosarcoma. No primary tumor was detected in any other organ. Within a few months the tumor had rapidly grown toward the soft tissue, and hemipelvectomy was performed. Examination of the surgical specimen revealed that the tumor was mainly composed of undifferentiated spindle sarcoma cells with scattered foci of chondrosarcoma and of squamous cell carcinoma with keratin pearl formation. The patient died approximately 6 months postoperatively. At autopsy multiple metastases were detected in the heart, both lungs, muscles, and lymph nodes. Interestingly, the chondrosarcoma and squamous cell carcinoma components were observed in several metastatic foci. The tumors in both the previously reported case and the present case contained components of chondrosarcoma and squamous cell carcinoma with keratin pearl formation, and this combination of histological features may be a unique characteristic of carcinosarcoma of bone.

Key words: bone, carcinosarcoma, chondrosarcoma, squamous cell carcinoma

Carcinosarcoma is defined as a tumor that contains both a carcinoma component and a sarcoma component, and carcinosarcomas generally occur in the genital organs, urinary systems, and digestive systems. Several different types of bone tumors, including adamantinomas and chordomas, exhibit epithelial features, but carcinomas do not usually originate in bone, and carcinosarcoma of bone is very rare. Only one previous case, a tumor with distinct carcinoma and sarcoma components, reported in 1986, has been documented.[1] That tumor was located in the humerus and was composed of chondrosarcoma and squamous cell carcinoma with keratin pearl formation. The subtypes in that case of the carcinoma and sarcoma component were the same as in the present case. Histological examination of tissue obtained at autopsy revealed the histological features of carcinosarcoma in several metastatic foci.

CLINICAL SUMMARY

A 53-year-old man complained of pain in his right thigh for 1 year, and osteomyelitis was suspected based on the plain radiography findings (Fig. 1a). Plain radiographs showed a mixed osteolytic and sclerotic change in the cortical border of the femoral diaphysis. Periosteal reaction was focally detected. The lesion had relatively distinct margin. Curettage revealed that the bone marrow was filled with whitish jelly-like material, and there was no apparent extraosseous proliferation. The curettage material was diagnosed as a grade 1 chondrosarcoma. The right thigh rapidly increased in size over the next few months, and massive growth toward the soft tissue around the femur was detected by scintigraphy and magnetic resonance imaging (MRI). Multiple small nodules were detected in both lungs on a computed tomography (CT) scan, and metastases were suspected. Hemipelvectomy was performed to secure a safe margin. After the operation, the patient received outpatient chemotherapy because he refused to be treated in the hospital. The chemotherapy regimen consisted of paraplatine (450 mg) once a month. Approximately 1 month later a cutaneous metastasis appeared on his face, and 2 months after that a second

Correspondence: Junichi Shiraishi, MD, Department of Diagnostic Surgical Pathology, Keio University, 35, Shinanomachi, Shinjuku-ku, Tokyo 160-8582, Japan. Email: jshira@chive.ocn.ne.jp

Received 29 November 2004. Accepted for publication 27 March 2005.

cutaneous metastasis appeared on his head. A large mass was detected in the right pulmonary artery on CT. The patient's respiration rapidly deteriorated and he died of respiratory failure approximately 6 months after the operation.

No primary lesion except the femur lesion was detected clinically or radiographically. The patient had no history of surgery or chemoradiation therapy prior to the amputation of his right thigh.

MATERIALS AND METHODS

The specimens of biopsy, operation and autopsy were fixed with 10% formalin and embedded in paraffin. Sections were cut 4 μm thick and stained with hematoxylin–eosin. The sections were also immunostained by the avidin–biotin–peroxidase complex method with antibodies to the cytokeratins (pancytokeratin; AE1 + AE3, monoclonal, mouse, DakoCytomation, Glostrup, Denmark, diluted 1:50 and high-molecular-weight keratin; 34βE12, monoclonal, mouse, Enzo Diagnostics, New York, diluted 1:20), epithelial membrane antigen (EMA; E29, monoclonal, mouse, DakoCytomation, diluted 1:200), S-100 protein (polyclonal, rabbit, DakoCytomation, diluted 1:200), desmin (D33, monoclonal, mouse, DakoCytomation, diluted 1:50), smooth muscle actin (1A4, monoclonal, mouse, DakoCytomation, diluted 1:100), and p53 (DO-7, monoclonal, mouse, DakoCytomation, diluted 1:20). Before staining for high-molecular-weight keratin, EMA and desmin, the sections were immersed in citrate buffer at pH 6.0 and placed in a microwave oven for 20 min. Before staining for p53, the sections were autoclaved in citrate buffer at 120°C for 15 min. Before staining for pancytokeratin, S-100 protein and smooth muscle actin, the sections were immersed in 0.1% tripsin at 37°C for 30 min.

PATHOLOGICAL FINDINGS

Curettage specimen

Histological examination of the curettage specimen revealed grade 1 chondrosarcoma (Fig. 2). The specimen consisted of irregularly shaped lobules or a less distinct lobular pattern and had a chondroid matrix. The cellularity was slightly increased, and the nuclei were enlarged and irregular in shape.

Operation specimen

Macroscopic examination of the surgical specimen revealed a whitish tumor measuring 25 × 14 × 13 cm with necrosis and hemorrhage, which was found in the upper and middle part of the right thigh. The destroyed femur was present at

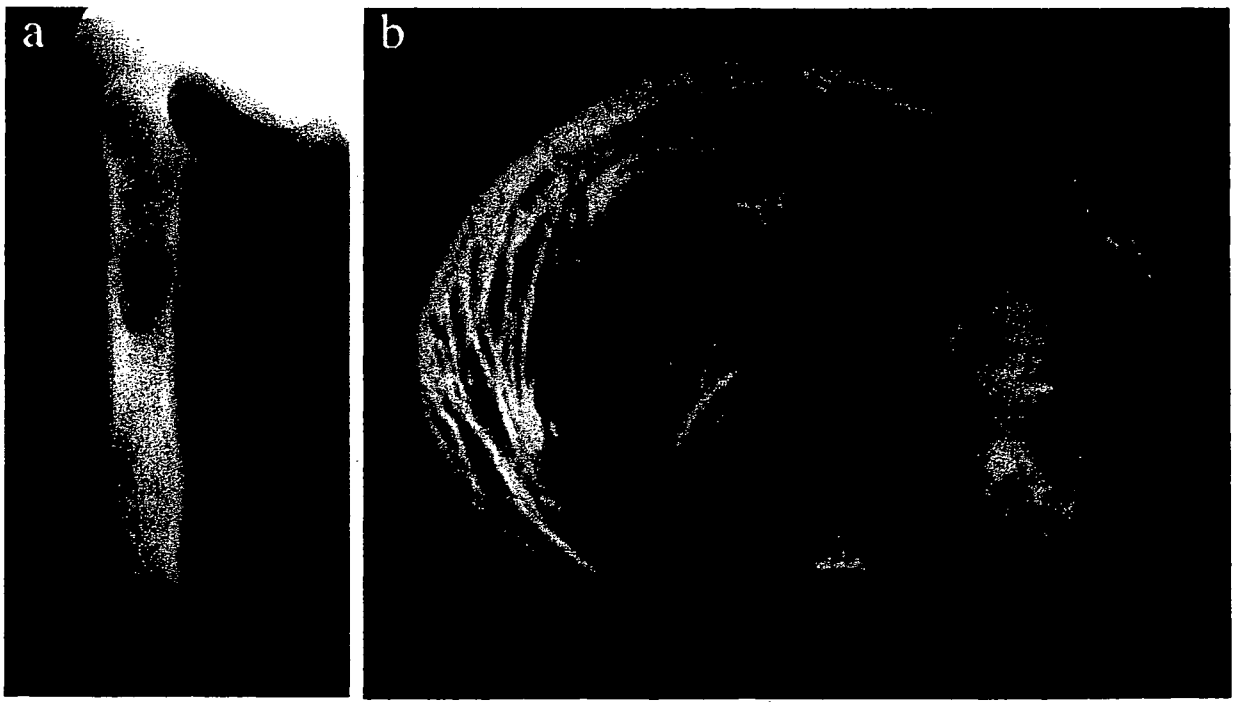

Figure 1 Plain radiograph and T2-weighted magnetic resonance imaging (MRI) of the right thigh. (**a**) Plain radiograph at the time of the first examination showed osteolytic change, sclerosis and periosteal reaction of the femur with no extra-osseous growth of a tumor. (**b**) MRI showed a huge tumor with massive extra-osseous growth.

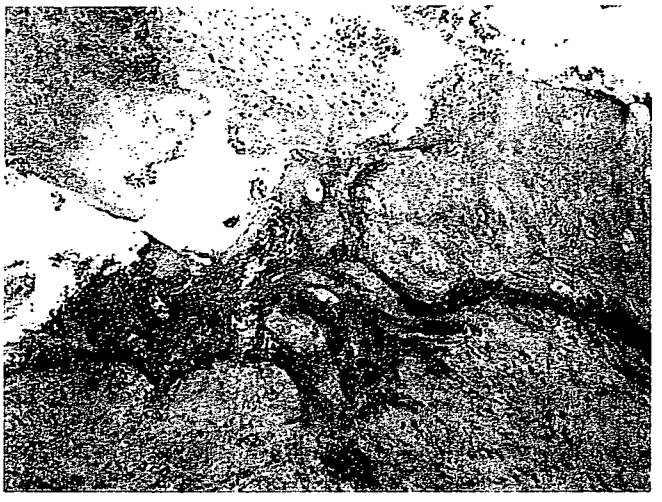

Figure 2 Curettage specimen diagnosed as grade 1 chondrosarcoma with irregularly shaped lobules and increased cellularity.

the center of the tumor (Figs 1b,3a). Several small foci of a chondroid nature were scattered throughout the intraosseous and extraosseous parts of the tumor. Microscopically, the tumor was mainly composed of undifferentiated spindle cell sarcoma with varying cellularity (Fig. 4a). These areas of spindle cell sarcoma were composed of plump or slender spindle cells containing abundant eosinophilic cytoplasm. The spindle cells were arranged in a haphazard, vaguely fascicular or storiform pattern, and they exhibited a moderate degree of nuclear pleomorphism and moderate mitotic activity. Small foci of grade 1 chondrosarcoma were found scattered throughout the tumor (Fig. 4b) as well as small-scattered foci of squamous cell carcinoma with prominent keratin pearl formation (Fig. 4d). The epithelial elements consisted of cancer nests that contained numerous cancer pearls. Occasionally small scattered foci of cancer pearls were seen in the component of spindle cell sarcoma. The areas of squamous cell carcinoma and the areas of chondrosarcoma each accounted for approximately 10% of the tumor. Spindle sarcoma cells were observed between the foci of chondrosarcoma and squamous cell carcinoma. No direct transitions from chondrosarcoma to squamous cell carcinoma were observed. There were no glandular structures or bone formation in the tumor. Immunohistological staining revealed that the squamous cell carcinoma areas were positive for epithelial markers (pancytokeratin and high-molecular-weight keratin, EMA; Fig. 4e), and the spindle cells adjacent to the squamous cell carcinoma foci were focally and weakly positive for epithelial markers. The chondrosarcoma areas were positive for S-100 protein (Fig. 4c), and the majority of the spindle cells were positive for vimentin, and negative for epithelial markers, S-100 protein, desmin, and smooth muscle actin. The surgical margin was negative for malignant cells. The spindle cell sarcoma component had metastasized to a lymph node adjacent to the

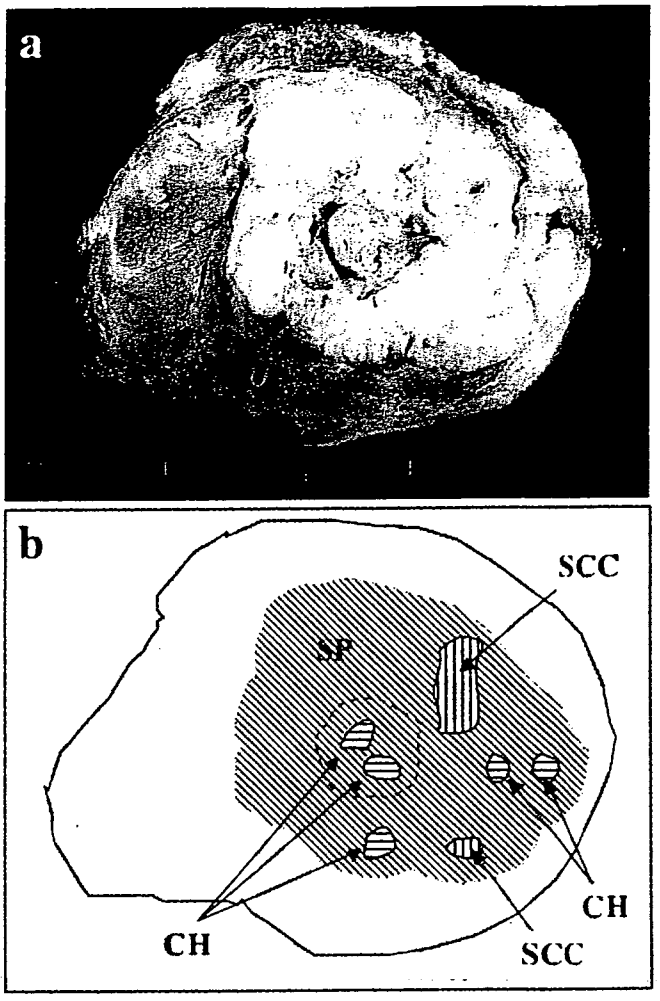

Figure 3 Macroscopic appearance of the cut surface and the schematic diagram of the tumor. (**a**) The tumor exhibited massive growth towards the soft tissue around the femur and had destroyed the femur. (**b**) Schematic diagram of each of the components of the carcinosarcoma on the same cut surface of (**a**). The tumor was composed of undifferentiated spindle cell sarcoma (SP), squamous cell carcinoma (SCC) and chondrosarcoma (CH). The dotted line in the tumor outlines a portion of the destroyed femur.

primary tumor, and the metastatic focus was negative for epithelial markers.

Autopsy specimen

A large, long whitish tumor was found in the area between the right atrium and the right pulmonary artery and was obstructing blood flow. Multiple metastases were observed in both lungs, the chest wall, the iliopsoas muscle, soft tissue in the pelvis adjacent to the bladder, and in the perigastric lymph nodes. Microscopic examination revealed that the metastatic foci consisted mainly of undifferentiated spindle cell sarcoma. A few foci of epithelial differentiation with trabecular arrangement were observed in the pulmonary metastases,

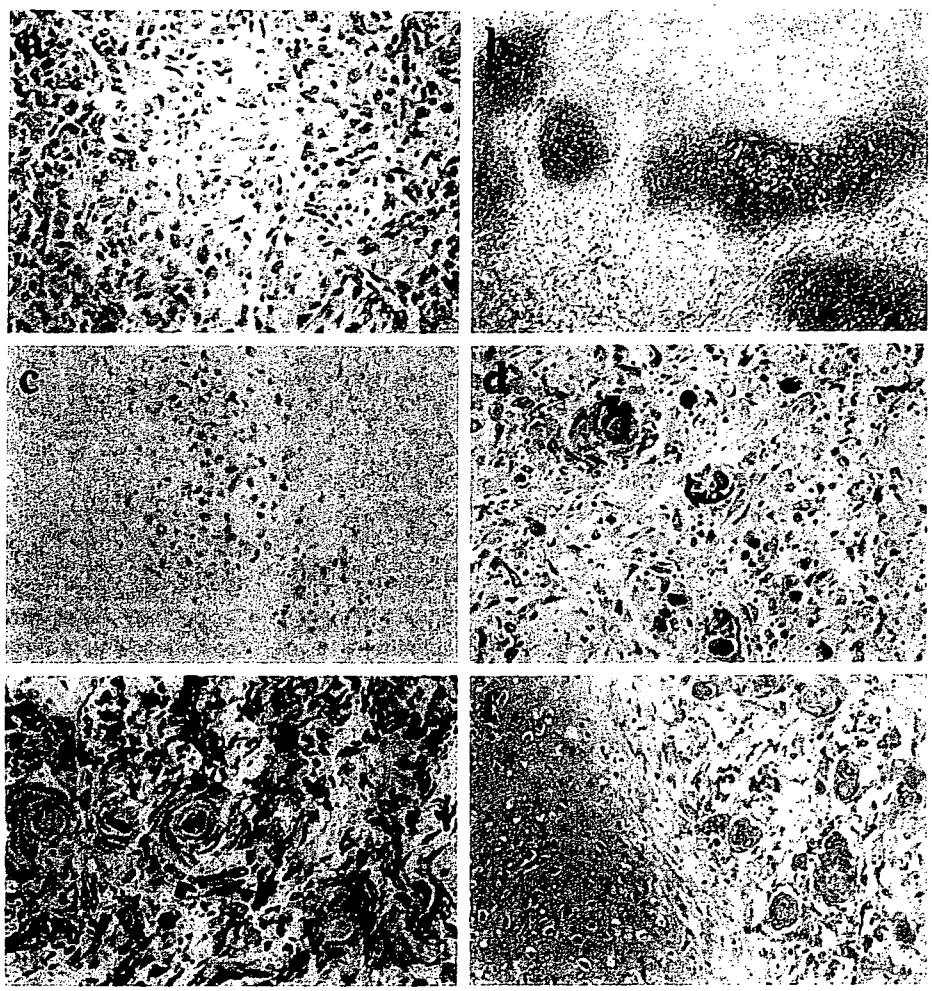

Figure 4 Microscopic appearance of the tumor. The main component of the tumor was (**a**) undifferentiated spindle cell sarcoma. (**b**) Chondrosarcomatous areas were scattered throughout the spindle cell sarcoma. (**c**) The chondrosarcomatous areas were positive for S-100 protein. (**d**) Foci of squamous cell carcinoma with prominent keratin pearl formation were occasionally observed in the spindle cell sarcoma. (**e**) The squamous cell carcinoma foci were strongly positive for pancytokeratin. (**f**) An area of squamous cell carcinoma is seen abutting against an area of chondrosarcoma in this intrapelvic nodule in the metastatic foci at autopsy.

an intrapelvic nodule and perigastric lymph nodes, and they were positive for epithelial markers. Small foci of chondrosarcoma and squamous cell carcinoma were also found in these metastatic lesions. It was particularly noteworthy that a squamous cell carcinoma component was found abutting against a chondrosarcoma component in an intrapelvic nodule (Fig. 4f). The direct cause of death was respiratory insufficiency secondary to tumor embolism.

DISCUSSION

Several cases of multipotential malignant neoplasms of bone have been reported.[2–4] They appeared to consist of undifferentiated cells with multiple differentiation (i.e. bone, cartilage, blood vessels, etc.). Hutter *et al.* proposed the term 'primitive multipotential primary sarcoma',[3] and Jacobson used the term 'polyhistoma' to describe sarcomas of bone that exhibit a broad mixture of histological types and represent multiple lines of differentiation.[4] A few cases of multipotential neoplasm with epithelial differentiation were documented in their reports. There have also been several reports of osteosarcoma and Ewing's sarcoma with epithelial differentiation, and the epithelial differentiation was confirmed by immunohistochemical or ultrastructural studies.[5–11] Primary bone tumors with definite epithelial differentiation, however, are extremely rare, and only one other case of a bone tumor containing definite squamous cell carcinoma and chondrosarcoma components has ever been reported.[1] Interestingly, the present case also contained components of chondrosarcoma and squamous cell carcinoma with keratin pearl formation.

Bone tumor with epithelial differentiation suggests the possibility of an adamantinoma, a rare primary bone tumor known to have an epithelial component. However, there were no components exhibiting a basaloid pattern or tubular pattern in the present case, and the prominent chondrosarcomatous component militated against a diagnosis of adamantinoma. A few cases of mixed tumor of bone have recently been reported, and because they contained a squamous component and a chondroid component[12,13] it was important to differentiate the present case from mixed tumor. Several findings in the present case indicated that it was not a mixed tumor of bone. First, there were no prominent myoepithelial cells or stellate cells. Second, all of the types of

tumor cells were glial fibrillary acidic protein-negative. The spindle cells in the present case were negative or weakly positive for smooth muscle actin immunohistochemically. And there were no tumors in the salivary glands at autopsy. Furthermore, the hypothesis of dedifferentiated chondrosarcoma with epithelial differentiation is considerable in the present case because the curettage material of femur revealed chondrosarcoma, and the operation material was mainly composed of undifferentiated spindle cell sarcoma. Several reports have been made of dedifferentiated chondrosarcoma with other mesenchymal components, such as rhabdomyosarcoma, angiosarcoma, osteosarcoma etc.; and one case of dedifferentiated chondrosarcoma containing a spindle cell area with intense cytoplasmic staining for cytokeratin has been documented.[14–18]

A biclonal and a monoclonal origin have been suggested to explain the histogenesis of two components of carcinosarcoma in many organs. Several molecular techniques have often been used to determine the histogenesis in different organs. In a few cases of carcinosarcoma the lesion was considered to be a biclonal tumor (collision tumor),[19–22] but most have appeared to be monoclonal. Thompson *et al.* determined the clonality of the carcinomatous and sarcomatous components of carcinosarcomas by examining a 511 bp region located within the first intron of the *human hypoxanthine-phosphoribosyl transferase* gene.[23] They demonstrated the comigration of the single homoduplexes generated by both carcinoma cells and sarcoma cells in six different organs. Gronau *et al.* determined the clonality to analyze for gains and losses of chromosomal material by comparative genomic hybridization and loss of heterozygosity analysis.[24] They demonstrated overlapping core aberration losses on the short arm of chromosome 9 and on the long arm of chromosome 11 in carcinosarcomas of the urinary bladder. Dacic *et al.* determined the clonality to perform an extensive comparative genotypic analysis in the six pulmonary carcinosarcomas.[25] Abeln *et al.* performed a loss of heterozygosity analysis in malignant mixed Mullerian tumors.[26] Emoto *et al.* showed that two clones established from a carcinosarcoma of the uterus were capable of differentiating into epithelial, mesenchymal, or both elements.[27] Kounelis *et al.* examined the point mutations in *p53* exons 5 through 8 in nine cases of female genital tract, and detected the loss of the wild-type allele in both carcinoma cells and sarcoma cells.[28] Wada *et al.* examined the mutation in the *p53* gene and *K-ras* gene, and found that the *p53* sequence was identical in both the carcinomatous and sarcomatous components of 21 carcinosarcomas of the uterus.[21] These results in several organs strongly support the theory of monoclonality of carcinosarcoma. In the present case each component must have been monoclonal, because the carcinoma and sarcoma components were intermingled in both the primary tumor and the metastatic lesions.

Two main hypotheses have been proposed to explain the differentiation of monoclonal tumor cells into separate epithelial and mesenchymal directions in carcinosarcoma. The first hypothesis is that both the epithelial and mesenchymal components are derived from totipotent (multipotential) stem cells,[1–3,23,25] and the second hypothesis is that the mesenchymal elements represent metaplastic change of epithelial elements.[22,26,29,30] These hypotheses are accepted in many organs, in which the most common malignant tumors are carcinoma. The hypothesis of totipotent stem cell is acceptable in all organs, including bone. In contrast, it is difficult to accept the metaplastic theory for primary bone tumors because there are no epithelial elements or primary carcinomas in bone tissue. Nevertheless, it is interesting that the combination of chondrosarcoma and squamous cell carcinoma has been observed in only two cases of primary bone carcinosarcoma with distinct epithelial differentiation: the present case and a previously reported case.

REFERENCES

1 Ling LL, Steiner GC. Primary multipotential malignant neoplasm of bone: chondrosarcoma associated with squamous cell carcinoma. *Hum Pathol* 1986; **17**: 317–20.

2 Frydman CP, Klein MJ, Abdelwahab IF, Zwass A. Primitive multipotential primary sarcoma of bone: a case report and immunohistochemical study. *Mod Pathol* 1991; **4**: 768–72.

3 Hutter RV, Foote FW Jr, Francis KC, Sherman RS. Primitive multipotential primary sarcoma of bone. *Cancer* 1966; **19**: 1–25.

4 Jacobson SA. Polyhistioma: a malignant tumor of bone and extraskeletal tissues. *Cancer* 1977; **40**: 2116–30.

5 Yoshida H, Yumoto T, Adachi H, Minamizaki T, Maeda N, Furuse K. Osteosarcoma with prominent epithelioid features. *Acta Pathol Jpn* 1989; **39**: 439–45.

6 Hasegawa T, Hirose T, Kudo E, Hizawa K, Usui M, Ishii S. Immunophenotypic heterogeneity in osteosarcomas. *Hum Pathol* 1991; **22**: 583–90.

7 Dardick I, Schatz JE, Colgan TJ. Osteogenic sarcoma with epithelial differentiation. *Ultrastruct Pathol* 1992; **16**: 463–74.

8 Hasegawa T, Shibata T, Hirose T, Seki K, Hizawa K. Osteosarcoma with epithelioid features. *Arch Pathol Lab Med* 1993; **117**: 295–8.

9 Kramer K, Hicks DG, Palis J *et al.* Epithelioid osteosarcoma of bone. Immunocytochemical evidence suggesting divergent epithelial and mesenchymal differentiation in a primary osseous neoplasm. *Cancer* 1993; **71**: 2977–82.

10 Moll R, Lee I, Gould VE, Berndt R, Roessner A, Franke WW. Immunocytochemical analysis of Ewing's tumors. Pattern of expression of intermediate filaments and desmosomal proteins indicate cell type heterogeneity and pluripotential differentiation. *Am J Pathol* 1987; **127**: 288–304.

11 Greco MA, Steiner GC, Fazzini E. Ewing's sarcoma with epithelial differentiation: fine structural and immunocytochemical study. *Ultrastruct Pathol* 1988; **12**: 317–25.

12 McGough RL, Wang LJ, Gnepp DR, Terek RM. Metastatic mixed tumor arising in bone. A case report and review of the literature. *J Bone Joint Surg Am* 2001; **83**: 1396–402.

13 Kamiyama K, Kinjo T, Chinen K *et al.* Aggressive mixed tumour, salivary gland type of the bone. *Histopathology* 2003; **43**: 408–10.
14 McCarthy EF, Dorfman HD. Chondrosarcoma of bone with dedifferentiation: a study of eighteen cases. *Hum Pathol* 1982; **13**: 36–40.
15 Johnson S, Tetu B, Ayala AG, Chawla SP. Chondrosarcoma with additional mesenchymal component (dedifferentiated chondrosarcoma). I. A clinicopathological study of 26 cases. *Cancer* 1986; **58**: 278–86.
16 Frassica FJ, Unni KK, Beabout JW, Sim FH. Dedifferentiated chondrosarcoma. A report of the clinicopathological features and treatment of seventy-eight cases. *J Bone Joint Surg Am* 1986; **68**: 1197–205.
17 Ishida T, Kuwada Y, Motoi N, Oka T, Machinami R. Dedifferentiated chondrosarcoma of the rib with a malignant mesenchymomatous component: an autopsy case report. *Pathol Int* 1997; **47**: 397–403.
18 Dervan PA, O'Loughlin J, Hurson BJ. Dedifferentiated chondrosarcoma with muscle and cytokeratin differentiation in the anaplastic component. *Histopathology* 1988; **12**: 517–26.
19 Sreenan JJ, Hart WR. Carcinosarcomas of the female genital tract. A pathological study of 29 metastatic tumors: further evidence for the dominant role of the epithelial component and the conversion theory of histogenesis. *Am J Surg Pathol* 1995; **19**: 666–74.
20 Iwaya T, Maesawa C, Tamura G *et al.* Esophageal carcinosarcoma: a genetic analysis. *Gastroenterology* 1997; **113**: 973–7.
21 Wada H, Enomoto T, Fujita M *et al.* Molecular evidence that most but not all carcinosarcomas of the uterus are combination tumors. *Cancer Res* 1997; **57**: 5379–85.
22 Seidman JD, Chauhan S. Evaluation of the relation ship between adenosarcoma and carcinosarcoma and a hypothesis of the histogenesis of uterine sarcomas. *Int J Gynecol Pathol* 2003; **22**: 75–82.
23 Thompson L, Chang B, Barsky SH. Monoclonal origins of malignant mixed tumors (carcinosarcomas). Evidence for a divergent histogenesis. *Am J Surg Pathol* 1996; **20**: 277–85.
24 Gronau S, Menz CK, Melzner I, Hautmann R, Moller P, Barth TF. Immunohistomorphologic and molecular cytogenetic analysis of a carcinosarcoma of the urinary bladder. *Virchows Arch* 2002; **440**: 436–40.
25 Dacic S, Finkelstein SD, Sasatomi E, Swalsky PA, Yousem SA. Molecular pathogenesis of pulmonary carcinosarcoma as determined by microdissection-based allelotyping. *Am J Surg Pathol* 2002; **26**: 510–16.
26 Abeln EC, Smit VT, Wessels JW, Leeuw WJ, Cornelisse CJ, Fleuren GJ. Molecular genetic evidence for the conversion hypothesis of the origin of malignant mixed mullerian tumours. *J Pathol* 1997; **183**: 424–31.
27 Emoto M, Iwasaki H, Kikuchi M, Shirakawa K. Characteristics of cloned cells of mixed mullerian tumor of the human uterus. Carcinoma cells showing myogenic differentiation in vitro. *Cancer* 1993; **71**: 3065–75.
28 Kounelis S, Jones MW, Papadaki H, Bakker A, Swalsky P, Finkelstein SD. Carcinosarcomas (malignant mixed mullerian tumors) of the female genital tract: comparative molecular analysis of epithelial and mesenchymal components. *Hum Pathol* 1998; **29**: 82–7.
29 Costa MJ, Khan R, Judd R. Carcinoma (malignant mixed mullerian [mesodermal] of the uterus and ovary. Correlation of clinical pathologic, and immunohistochemical features in 29 cases. *Arch Pathol Lab Med* 1991; **115**: 583–90.
30 Humphrey PA, Scroggs MW, Roggli VL, Shelburne JD. Pulmonary carcinomas with a sarcomatoid element: an immunocytochemical and ultrastructural analysis. *Hum Pathol* 1988; **19**: 155–65.

厚生労働省科学研究費補助金
基礎研究成果の臨床応用推進研究事業

ヒト化CD26抗体の難治性免疫疾患
（クローン病、GVHDなど）への治療法開発

平成１７年度～平成１９年度
総合研究報告書

平成20年4月10日発行

発行：主任研究者　森本　幾夫
〒108-8639 東京都港区白金台 4-6-1
TEL:03-5449-5546

東京大学医科学研究所
先端医療研究センター 免疫病態分野